Substructuring with Nonlinear Subcomponents: A Nonlinear Normal Mode Perspective

Matthew S. Allen
&
Robert J. Kuether
Department of Engineering Physics
University of Wisconsin
Madison, WI 53706
msallen@engr.wisc.edu, rkuether@wisc.edu

ABSTRACT

Substructure coupling techniques allow one to predict the response of an assembly from dynamic models for each subcomponent. Linear substructures are routinely used in analysis (e.g. the Craig-Bampton method) to reduce the computational cost of vibration, noise and load predictions for structures. They also provide a designer with insight into the influence that each subcomponent has on the assembled system's natural frequencies, mode shapes and damping. These concepts are currently limited to assemblies of linear substructures. This work explores substructuring with nonlinear subcomponents (substructures), using the nonlinear normal modes of each substructure to seek to understand how those contribute to the nonlinear modes of the assembly. The goal is to extend the insights that have been developed over the past several years for linear substructures, to nonlinear ones. A specific type of describing function model, which captures the variation of the structure's natural frequencies and mode shapes with energy is introduced, which is here dubbed a Representative Linear Modal Model (RLMM). The results show that this type of model can be used with linear substructuring techniques to effectively predict the dynamics of a nonlinear assembly, suggesting that linear substructuring concepts may be applied advantageously to nonlinear assemblies.

1. Introduction

Dynamic substructuring techniques allow one to predict the dynamics of an assembly from knowledge of the dynamics of each subcomponent and the way in which the subcomponents are assembled. For example, this is the basis of the finite element method, where individual elements with known stiffness and mass are assembled to approximate the behavior of a complicated structure. However, substructuring methods are more often employed in situations in which the subcomponents are more meaningful, for example, models of an engine and transmission may be assembled to predict the performance of a vehicle's powertrain. In applications such as this each subcomponent is likely to be described by a reduced order model. For example, when the subcomponents are linear, their low frequency modes (e.g. a Craig-Bampton model [1]) can be used to construct a reduced order model for each subcomponent and then dynamic substructuring procedures can be used to assemble the system; more simply, this approach allows one to predict the modes of an assembly from the known modes of the subcomponents. These techniques are also valid when the model for one of the subcomponents is derived experimentally (i.e. instead of using the finite element method to create the reduced-order modal model). Substructuring techniques are quite mature for linear assemblies comprised of analytical (e.g. Finite element) subcomponents, while, on the other hand, they are still not used very frequently with experimentally derived models. Work is ongoing in this area [2-4]. The reader is referred to a recent review [5] for additional details.

Substructuring methods can be classified as to whether they use modal models for the subcomponents, termed Modal Substructuring, or, for linear systems, the frequency response functions, called Frequency Based Substructuring in [5]. Modal substructuring will be the focus of this work. The concept of modes is very powerful. For example, one can show that each mode of an assembly is most strongly affected by those subcomponent modes that have similar frequencies [6] (or see the case study in [7]), so if an assembly has a mode at an undesirable frequency a designer can target specific subcomponent motions to alleviate the problem. Modes

can also be used to construct very efficient subcomponent models. For example, while it may be prohibitively expensive to compute the modes of a structure that is modeled by millions of finite elements, the computational cost can be reduced dramatically by first breaking the substructure into subcomponents, using the Craig-Bampton method to construct modal models of each and then assembling the reduced-order models. Modal models are also convenient when a substructure is modeled experimentally, since the modes of the structure are readily manifest in the response and can be extracted to create a compact model for the subcomponent.

This work seeks to extend the concept of modal substructuring to nonlinear dynamic systems. A nonlinear system does not have modes if one remains bound to the classical definition, but many of the key concepts can be readily extended to nonlinear systems using the concept of a nonlinear normal mode (NNM). Specifically, a nonlinear normal mode describes the frequency of oscillation and the deformation shape of a nonlinear structure, and how those evolve with increasing energy (or amplitude). Here the definition pioneered by Rosenberg [8] will be used, which was developed further in recent years by Vakakis, Kerschen and others [9-11]. This work explores the relationship between the nonlinear normal modes of an assembly and those of its subcomponents, revealing that many concepts from linear substructuring can be readily extended to nonlinear systems. For example, this work shows that two nonlinear subcomponents with similar NNM frequencies interact to form new modes at distinct frequencies in the assembly, in much the same way that two linear modes combine in the classical vibration absorber.

The concept of modes with amplitude or energy dependent frequencies, which is central to this work, is well established although perhaps only more recently placed on a firmer theoretical basis using the nonlinear normal mode concept. (The concept of frequency energy dependence will be rigorously defined in Section 2.3.) For example, many structures are only weakly nonlinear so that the nonlinearity is thought to have little effect besides causing the effective natural frequencies and/or mode shapes to change somewhat as the forcing amplitude is increased. Hence, it has often been suggested that one can simply ignore the nonlinearity and obtain adequate accuracy with a linear model so long as the appropriate natural frequency (for the forcing level of interest) is used when simulating the response or performing substructuring. (See, for example [12]. This idea is also closely related to the describing function approach used in nonlinear controls [13], also called quasi-linearization.) This work explores the validity of this approach and seeks to understand its merits and limitations with regard to substructuring. The results presented here suggest that this approach is remarkably useful. The examples presented show that the amplitude dependent modal parameters of two subcomponents can be combined with linear modal substructuring to accurately predict the frequency-energy evolution of the nonlinear normal modes of the assembly. This approximate substructuring approach could be very valuable when designing systems with nonlinear subcomponents, since it allows the analyst to predict how the NNMs of an assembly will react to a structural modification.

The paper is organized as follows. The following section briefly reviews substructuring theory for both linear and nonlinear systems. Then the nonlinear normal mode concept is introduced and explained in this context. An approximate substructuring method is then proposed in Section 2.4, which reveals how changes in the effective frequency and mode shape of a nonlinear subcomponent affect those of the assembly. The proposed methods are demonstrated on some relatively simple, nonlinear, spring-mass models in Section 3 and the conclusions are presented in Section 4.

2. Theory

2.1 Review of Substructuring Theory for Linear and Nonlinear Systems

Figure 1 shows a schematic of a general substructuring problem, adapted from [5], where two substructures, denoted A and B, are assembled at three connection points in order to form the built-up system.

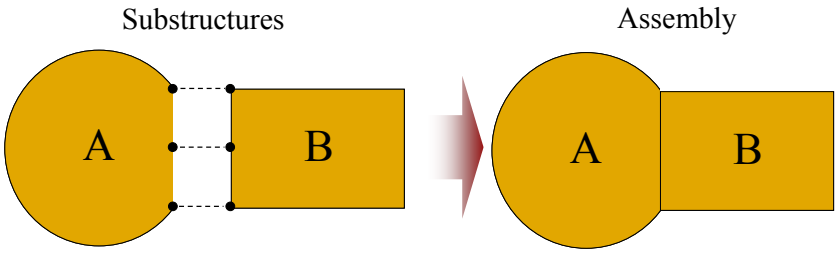

Figure 1: Schematic of general substructuring problem. Subcomponents A and B are assembled at a series of connection points to form the assembly of interest.

A general, nonlinear dynamic system can be described with the following equation of motion in terms of the state vector, **x**, and the input forces, **u,** which are comprised of both the forces applied at the interface (i) and elsewhere (app) $\mathbf{u}(t)=\mathbf{F}^{A}_{i}+\mathbf{F}^{A}_{app}$. The superscript $()^{A}$ identifies the quantities that pertain to substructure A and similarly for B.

$$\begin{aligned}\dot{\mathbf{x}}^{A}(t)&=\mathbf{f}^{A}\left(\mathbf{x}^{A}(t),\mathbf{u}(t)\right)\\ \dot{\mathbf{x}}^{B}(t)&=\mathbf{f}^{B}\left(\mathbf{x}^{B}(t),\mathbf{u}(t)\right)\end{aligned} \tag{1}$$

The derivative of the state vector is, in general, a nonlinear function, $\mathbf{f}^{A}()$, of the states and the input forces. A similar set of equations is written for B and the process could be repeated for any number of subcomponents. The goal is to assemble the subcomponent models in order to obtain a dynamic model for the built-up system.

Assembly is accomplished by enforcing equal displacement at certain points, e.g. $\mathbf{x}^{A}_{1}=\mathbf{x}^{B}_{3}$ if the first node of A is joined to the third node of B. Common constraints are linear and can be written as follows

$$\mathbf{a}\begin{Bmatrix}\mathbf{x}^{A}\\ \mathbf{x}^{B}\end{Bmatrix}=\mathbf{0} \tag{2}$$

Where **a** is a matrix of constants, e.g. for the case where the constraint is $\mathbf{x}^{A}_{1}=\mathbf{x}^{B}_{3}$, **a** is a row vector with a value of 1 in the first column and with -1 in the column corresponding to $\mathbf{x}^{B}_{3}$. The state vector contains both displacements and velocities, but typically only the displacements need to be constrained. One must also enforce equilibrium, or in other words that the net force at each point on the interface should be zero after assembly (assuming that no external forces are applied at the interface).

Equations (1) and (2) constitute a set of differential-algebraic equations (see Ginsberg [14]) or constrained ordinary differential equations, since the state vector is not free to assume any value for each state but must satisfy Eq. (2). Equations such as these can be solved by various methods. When the substructures are linear one typically uses Eq. (2) to eliminate some of the states in order to form an unconstrained set of generalized coordinates (see [15] or [5]). The basic linear substructuring process is summarized in Figure 2 below. Further mathematical details are provided in the Appendix.

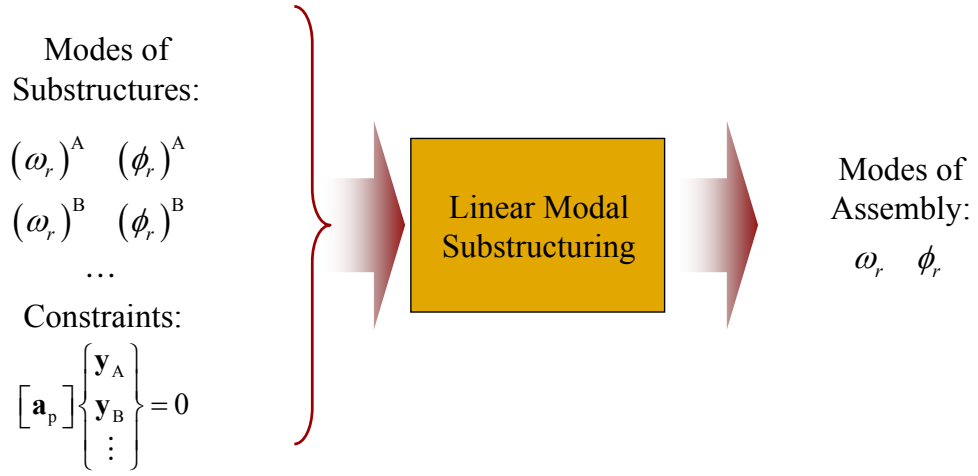

Figure 2: Overview of linear modal substructuring process. Modal models for the substructures are combined, constraints are enforced between the components, and the result is an estimate of the mode shapes and natural frequencies of the assembly.

2.2 Linearization

It is important to contrast the approach that shall be presented in this work with linearization. One can use the Taylor series expansion of the equations of motion in Eq. (1) to obtain the following linearized system,

$$\dot{\mathbf{x}}^A(t) = \mathbf{A}\mathbf{x}^A(t) + \mathbf{B}\mathbf{u}(t)$$
$$\mathbf{A} = \left[\frac{\partial \mathbf{f}_i}{\partial \mathbf{x}_j}\right]_{\bar{\mathbf{x}},\bar{\mathbf{u}}}, \quad \mathbf{B} = \left[\frac{\partial \mathbf{f}_i}{\partial \mathbf{u}_j}\right]_{\bar{\mathbf{x}},\bar{\mathbf{u}}} \tag{3}$$

where the notation signifies that the (i,j)th element of the A matrix is the derivative of the ith function in **f** with respect to the jth element of **x** (see [16] for further details). Note that the Jacobians must be evaluated at a fixed value of the state and input, $\bar{\mathbf{x}}, \bar{\mathbf{u}}$, to obtain a linear time invariant model. One could evaluate the Jacobians at every point along a trajectory but then a time-varying model would be obtained. (See, e.g. [17].)

This derivation reveals that one cannot obtain a linear time invariant model for a system by linearizing about a certain amplitude or input level. Only the mean value of the displacement or forcing may be varied if one wishes to obtain a rigorous linear time invariant model. However, in many applications of interest the resonance frequencies of a structure seem to change in response to the amplitude of the forcing or response, but an alternate methodology is needed to describe this phenomenon.

2.3 Undamped Nonlinear Normal Modes (NNMs)

While a few definitions exist for nonlinear modes, the definition that will be used here is that a nonlinear normal mode (NNM) is simply a vibration in unison of a system or a "not necessarily synchronous periodic solution" to the equations of motion [9]. This definition is essentially the same as the definition of a linear mode, since linear modes are also found by solving for the periodic solutions of the linear equations of motion. However, there are several important differences the most significant being that the response of a nonlinear system is not a linear superposition of its nonlinear normal modes. Vakakis provided an excellent review of the literature in this area, explaining how NNMs relate to the response of the system and highlighting methods for finding them analytically [10]. Kerschen also recently provided an excellent overview [9].

It is helpful to illustrate the nonlinear normal mode concept with a single-degree-of-freedom (SDOF) system before proceeding. Figure 3 shows the fundamental frequency of the NNM of a Duffing oscillator whose equation of motion is given below in nondimensional form. The parameters used in this example are: ζ=0.01, ω_1=1 and ω_3=0.5.

$$\ddot{x} + 2\zeta\omega_1\dot{x} + \omega_1 x + \omega_3 x^3 = f(t) \tag{4}$$

The NNM is merely a periodic solution to the undamped (ζ=0) equation of motion for the system; so if the system were linear then a possible periodic solution would be a pure sinusoid at a specific natural frequency, with a certain magnitude and phase. The analogous solution to the nonlinear equation of motion is a fundamental frequency plus a series of harmonics. Figure 3 shows how the fundamental frequency of this solution evolves as the total energy in the system increases. The black line gives the fundamental frequency of the response, or frequency of the NNM, at each energy level. As expected for this system (whose nonlinearity is of the hardening type) the fundamental frequency increases as the energy increases. For example, if the undamped system were given an initial energy of E = 10^2 (dimensionless) and released, the system would oscillate at a fundamental frequency of 2.7 rad/s. It is clear that the NNM concept captures how the oscillation frequency of structure may change with amplitude. For convenience, the nonlinear normal mode frequency of the *r*th mode will be denoted $\omega^{\mathrm{NNM}}(E)_r$, where the dependence on energy is explicit noted, or more simply, $\omega^{\mathrm{NNM}}{}_r$. Note that the NNM frequency may be multi-valued, that is, the NNM curve may fold back so that there are several possible frequencies for *r*th NNM at certain energy levels; this is termed an internal resonance of the nonlinear system and will be observed in the example in Section 3.

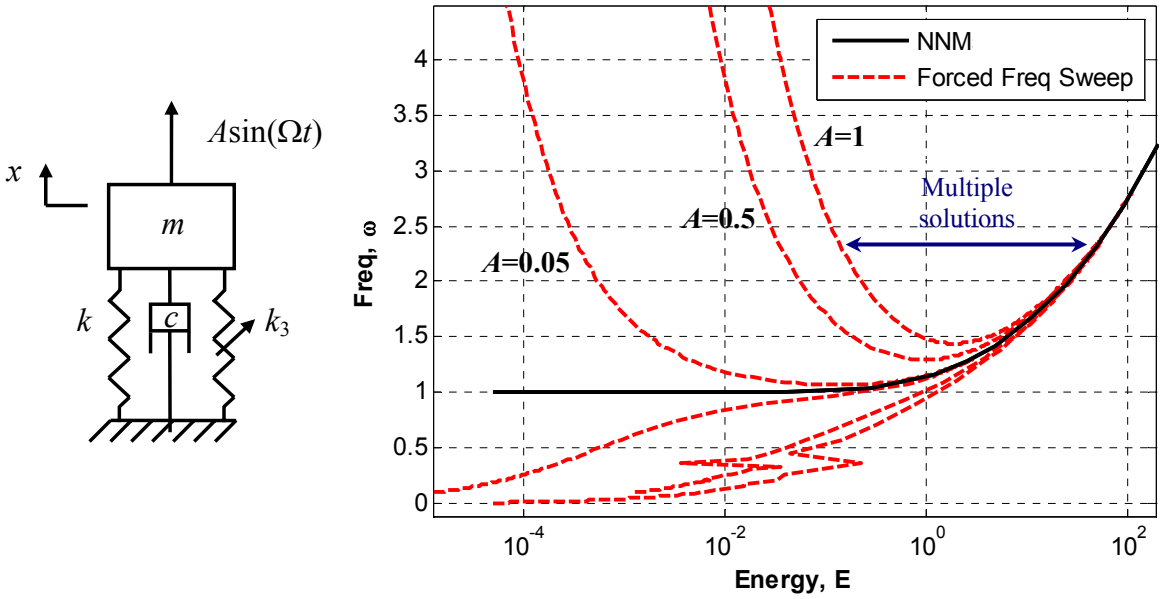

Figure 3: (solid black) Frequency-energy plot for the nonlinear normal mode of a single-degree-of-freedom Duffing oscillator. (dashed red) Frequency response curves of Duffing oscillator at various forcing amplitudes. The NNM provides tremendous insight into the free and forced response of the system.

The NNMs of a system are closely related to its forced response, analogous to the way in which the linear modes can be used to explain the forced response of a linear system (see, e.g. [10]). The red curves in Figure 3 show the forced response of the Duffing oscillator at different excitation levels. Contrary to the usual convention, frequency is on the vertical axis in this figure. The curves for nondimensional forcing amplitudes A = 0.05, 0.5 and 1.0 are shown, all computed with ζ = 0.01. The NNM forms the backbone of the frequency response curves, which reach further up the NNM as the amplitude increases. At high enough amplitude, the frequency response curves bend upward and a region emerges where three possible solutions exist (i.e. three possible response amplitudes for a fixed forcing frequency and amplitude). One of the solutions is unstable, but either the other might be observed at that forcing level, depending on the structure's initial conditions. One can also see that peaks begin to emerge at lower frequencies as the amplitude increases. These peaks occur at integer fractions of the NNM frequency and correspond to superharmonic resonances of the system [18]. Nonlinear normal modes and nonlinear forced response curves such as these are relatively straightforward to compute using recently developed continuation techniques, and they provide tremendous insight into the dynamics of the system. The nonlinear mode of the Duffing oscillator shown above was found using the methods in [9, 11] implemented in

their "NNMcont" Matlab package. The nonlinear frequency response curves were computed using the closely related method that is described in [19].

The nonlinear normal modes of a system depend on its nonlinear stiffness and mass, in much the same way that the linear modes of a structure depend on its linear stiffness and mass. For example, Figure 4 shows how the NNM of the Duffing system changes as (a) its nonlinear stiffness increases from 0.5 (black line) to 0.75 1.0 1.25 and 1.5, (b) its linear stiffness increases from 1.0 (black line) to 1.25 1.5 1.75 and 2.0 or (c) its mass increases from 1.0 (black line) to 1.25 1.5 1.75 and 2.0. The behavior of the NNM is quite intuitive in this simple example. The changes in the frequency at low energy due to increasing the mass and stiffness are exactly what one would predict with linear theory.

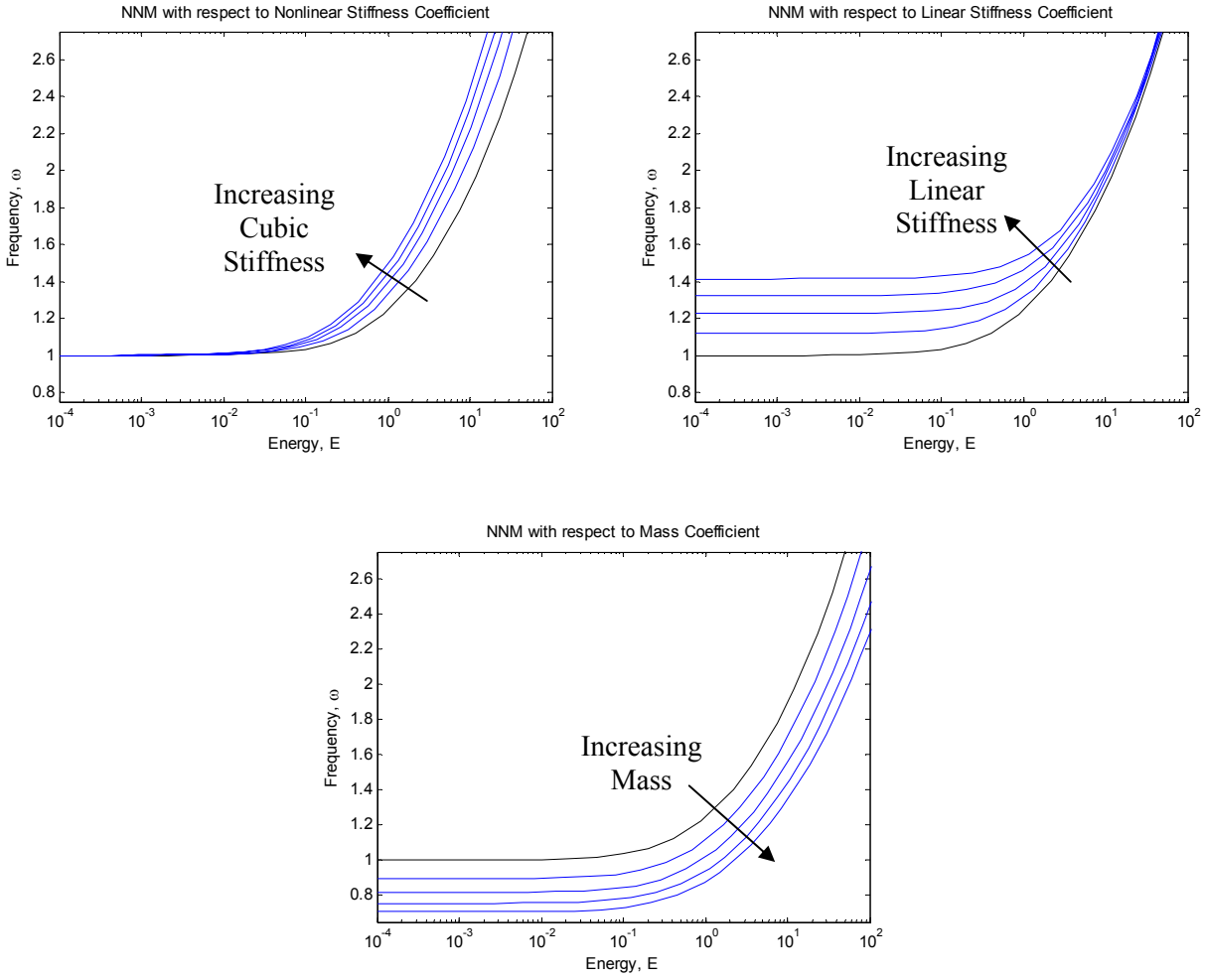

Figure 4: Frequency-energy plots for the nonlinear normal mode of the single-degree-of-freedom Duffing oscillator. (Black) Reference NNM curve (same as in Figure 3). (Blue) Changes in NNM frequency with mass, linear stiffness and nonlinear stiffness.

When a system possesses multiple degrees of freedom, there are several nonlinear normal modes. Each mode can be characterized by a frequency-energy backbone curve such as that shown above for the Duffing oscillator. As with a linear mode, the structure also exhibits a particular deformation shape during each NNM. When a linear structure vibrates in a linear modal motion, the deformation of the structure can be written as

$$\mathbf{x} = \begin{bmatrix} \phi_{1r} & \phi_{2r} & \cdots & \phi_{Nr} \end{bmatrix}^{\mathrm{T}} q_r = \boldsymbol{\varphi}_r(q_r) \tag{5}$$

where q_r is the amplitude of the rth mode of vibration and ϕ_{jr} is the shape of the rth mode at the jth node. One could also think of the mode shape as expressing a functional relationship between all of the nodes of the structure

and the modal amplitude, q_r, so one could write the structural deformation as a vector function $\boldsymbol{\varphi}_r(q_r)$. In the case of a linear system as shown above, each element of the function $\boldsymbol{\varphi}_r(q_r)$ is simply proportional to, or a linear function of q_r. As one might expect, when the system is nonlinear the NNMs become nonlinear functions of the modal displacement. For example, Figure 5 shows the shape, in the (x_1,x_2) space, of the first nonlinear normal mode of a two-DOF system that is described later (shown in Figure 7). It is clear that x_2 and x_1 are nonlinear functions of the amplitude. If the system were linear, the relative amplitudes would obey a linear trend as is shown with the dashed red line.

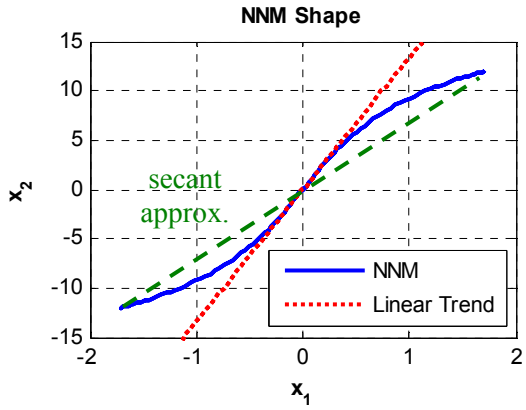

Figure 5: Shape of the 1st NNM of the system shown in red in Figure 7 at E = 13.2.

A NNM shape such as that shown with a blue line in Figure 5 is only valid for a single energy level. Hence, the *r*th NNM of a nonlinear system will here be denoted $\boldsymbol{\varphi}^{\mathrm{NNM}}(E,q_r)_r$ to make the dependence on energy explicit, or more simply, $\boldsymbol{\varphi}^{\mathrm{NNM}}{}_r$. It is important to note that the NNM curve at a low energy is not necessarily a subset of the NNM at a higher energy. For example, if a second curve was added to Figure 5 showing the NNM at a higher energy level, the two curves would not generally overlay. Also, in some situations the modal amplitude is a complicated function of the physical displacements, so it is often more convenient to write the NNM shape as a function of time $\boldsymbol{\varphi}^{\mathrm{NNM}}(E,t)_r$, where time is only defined within the fundamental period $0 \le t < 2\pi/\omega^{\mathrm{NNM}}(E)_r$.

2.4 Proposed Approximate Nonlinear Substructuring Methodology Based on Representative Linear Modal Models (RLMMs)

At the most basic level, one can think of a nonlinear normal mode as providing the frequency and mode shape of a system as a function of energy. As explained in the previous section the NNM shapes are not simple linear functions of modal amplitude and the frequency of the NNM is only the fundamental frequency of a multi-frequency oscillation. In any event, this leads one to question: To what degree is the behavior of the nonlinear system well described simply by the change in the fundamental frequency of oscillation of the nonlinear system with energy? If the system can be described by a linear model with the appropriate frequency and mode shape then modeling, simulation and test could all be simplified dramatically. Section 2.2 established the fact that linearization will not generally capture a nonlinear system's frequency-energy dependence. Here an alternative description is proposed based on the nonlinear normal mode concept and which is dubbed a Representative Linear Modal Model (RLMM). This concept is closely related to the describing function concept, which has various definitions and uses [13, 20].

A representative linear modal model is a linear system defined by a set of natural frequencies and mode shapes, both of which are functions of energy. The RLMM natural frequency, $\omega^{\mathrm{R}}(E)_r$, is taken to be the fundamental frequency of the NNM curve of the system.

$$\omega^{\mathrm{R}}(E)_r = \omega^{\mathrm{NNM}}(E)_r \tag{6}$$

In cases where the NNM frequency is multi-valued one could retain the various values, or simply select a single branch of interest and discard the others. The mode shape might be obtained in a number of ways. In this work we propose to use a secant approximation to the NNM. Specifically, the mode shape is taken to be the maximal deformation of the structure, defined as the deformation at the instant when the velocity is zero (assuming a predominantly synchronous motion),

$$\phi^{\mathrm{R}}(E)_r = \boldsymbol{\varphi}^{\mathrm{NNM}}(E, t_{\mathrm{dpk}})_r \tag{7}$$

where t_{dpk} is the time instant at which $\dot{\mathbf{x}} = 0$. At a particular energy level the mode shape is a vector of constants akin to a linear mode shape. For example, consider the NNM shape shown in Figure 5. The maximal deformation occurs at the extremes of the blue curve, so the proposed RLMM mode shape approximates the NNM with a line connecting the maximum positive and negative deformations of the structure, or a secant line connecting the two extremes of the NNM shape.

The goal in defining representative linear modal models is to characterize the response of the nonlinear system and to facilitate substructuring predictions when various subcomponents are assembled. Towards the latter goal, this work proposes to treat the RLMMs of two subcomponents as linear models. Hence, given the RLMMs of two subcomponents at various energy levels, one would simply use linear modal substructuring techniques to predict the modes of the assembly. The resulting modes of the assembly would then be an RLMM model describing the frequency-energy and mode shape-energy dependence of the assembled system. The procedure is outlined in Figure 6 and specific examples will be presented in the following section.

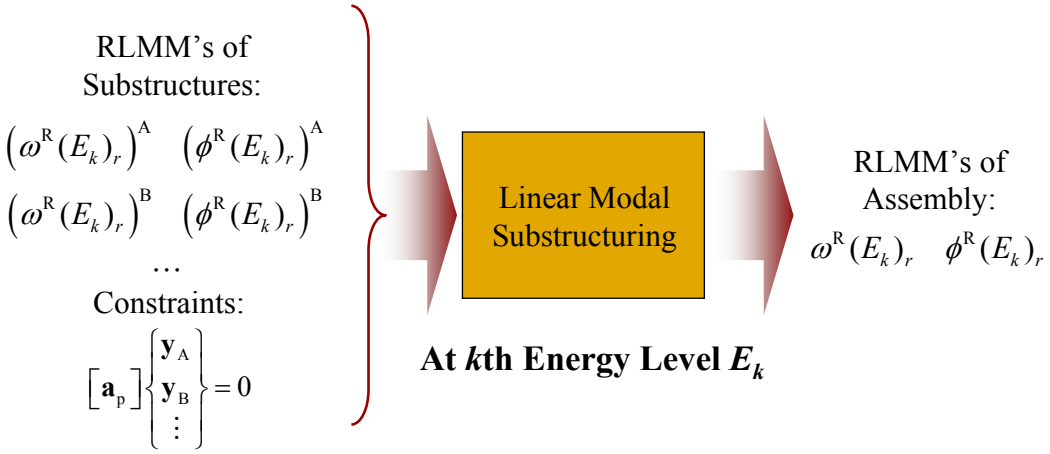

Figure 6: Overview of the proposed approximate substructuring procedure based on representative linear modal models for each subcomponent.

It is interesting to contrast this approach with a complete nonlinear model for the assembly. For example, Apiwattanalunggarn Shaw, and Pierre [21] adapted the Craig-Bampton approach to accommodate nonlinear normal mode models, but found that it was quite impractical to compute nonlinear normal modes that contained the required nonlinear couplings and also to simulate the response of the assembly using the NNM subcomponent models. In contrast, the operations outlined in Figure 6 could be performed at negligible computational cost even if each subcomponent has dozens of RLMMs.

3. Case Study

The fundamentals of nonlinear substructuring will be explored with the simple substructuring problem that is depicted in Figure 7, where two nonlinear spring-mass systems are joined forming a 2DOF built-up system. The parameters used are: m_1=1, m_2=0.5, m_3=0.5, k_1=1, k_2=0.2, and the nonlinear springs are cubic with coefficients $k_{\mathrm{nl},1}$=0.5 and $k_{\mathrm{nl},2}$=1e-5. The figure shows the frequency-energy dependence of the nonlinear normal modes of each of the subcomponents, as well as those of the assembled system. The NNMs of the assembled system were computed directly from the model for system C shown below; there was no approximation of the system so these NNMs can be taken to be the truth model for the nonlinear system.

This system is linearizable, so it is helpful to first consider what insights the linearized system provides. Each NNM of the system reduces to the linearized natural frequency of the structure at sufficiently low energy (at the far left edge of the plot). The system parameters are such that the linearized natural frequency of the base system, A, (blue line) is ω^A_1=1 rad/s, which is close to the second linearized natural frequency, $\omega^B_2=(2k_2/m_2)^{(1/2)}\approx 0.89$, of the attached system, B, (green line). (Note that $\omega^B_1=0$.) The dashed red lines in Figure 7 give the natural frequencies obtained by combining the linearized models ($k_{nl,1}= k_{nl,2}=0$), revealing that the two modes of the subcomponents that have similar natural frequencies combine to form two new modes of system C that have distinct natural frequencies. This is similar to the standard vibration absorber or mass-tuned damper problem (see, e.g. [22]), where the two modes of the subcomponents combine to form two new modes, one above and the other below the original resonance frequency.

3.1 Rigorous Analysis of the Nonlinear Assembly

Now consider the nonlinear system. At low energy the subcomponents are well approximated as linear and the linearized analysis predicts their natural frequencies precisely. As energy increases, the NNM of subsystem A increases in frequency, beginning at an energy of E=0.1. Subsystem B has a weaker nonlinearity ($k_{nl,2}$ is four orders of magnitude smaller than $k_{nl,1}$), so its NNM frequency does not begin to increase until E=100. Interestingly, the two NNMs of the assembly, C, seem to track the frequencies of subsystems A and B, with the higher NNM of C following the curve for system A's nonlinear mode and the lower one following the curve for B's nonlinear mode.

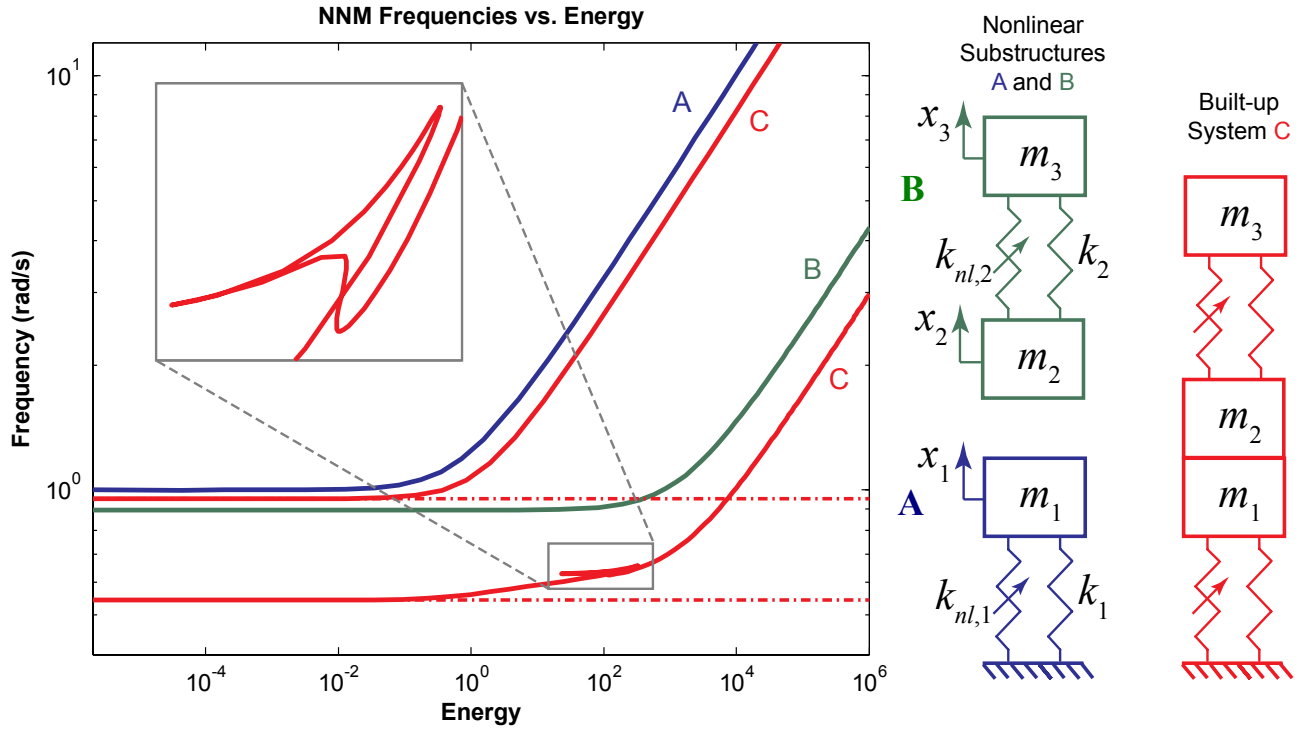

Figure 7: (right**) Simple substructuring problem where a nonlinear SDOF system is coupled to a nonlinear 2DOF system. The system is assembled, as shown on the far right, by enforcing the constraint x_1=x_2. (**left**) Plot showing frequency versus energy dependence of the nonlinear normal modes of the subcomponents (blue and green lines) and of the assembled system (red). At low energy the NNMs of the assembled system converge to the frequencies predicted by a linear analysis (dashed red lines).**

Viewing the substructuring problem in terms of nonlinear normal modes in this manner leads to a number of important insights. First, it seems that the first NNM of the built-up structure is primarily influenced by the nonlinear mode of subsystem B. The NNM of subsystem A seems to dominate the second NNM of the assembly. This information can be very valuable during the design process. For example, if the response analysis were to

reveal that the 1st NNM of the assembled system was responsible for excessive vibration, then one might target the NNM of subsystem B in order to cause the greatest change.

The inset in Figure 7 shows a magnified view of the 1st NNM frequency over a small range of energy, revealing a feature which is unique to nonlinear systems. The natural frequency of the first NNM is seen to change in a very erratic way at this energy level. The mode shape also changes dramatically in this region (not shown) as the system exhibits a 1:3 internal resonance (the first mass moves at 3 times the frequency of the second). This type of response could be detrimental, since it could lead to high vibration levels at unexpected frequencies. On the other hand, this phenomenon has also been proposed as a mechanism for very effective nonlinear vibration absorbers [23]. It is also important to note that one could have predicted that subharmonic resonance was possible at this energy level because the 2nd NNM frequency is three times the 1st NNM frequency at that energy and the nonlinearities are cubic. The NNM frequency-energy dependence of the coupled system seems to follow the trend of the individual subcomponent NNMs except in this relatively small region where this internal resonance occurs.

3.2 Substructuring Analysis with Representative Linear Modal Models

The frequency-energy plot in Section 3.1 presented the true dynamics of the assembly of nonlinear subcomponents. This section considers the result that one obtains using RLMMs for the substructures A and B. Substructure A is a single degree-of-freedom system, so it has a single nonlinear mode whose frequency-energy dependence, $\left(\omega^{\mathrm{R}}(E)_1\right)^{\mathrm{A}}$, is shown with a blue line in Figure 7, ranging from 1 rad/s at low energy to 17.8 rad/s at E=10^5. The corresponding nonlinear mode shape is a scalar value which, after mass-normalizing, remains unchanged, $\left(\phi^{\mathrm{R}}(E)_1\right)^{\mathrm{A}} = 1$. Substructure B is a two degree-of freedom system, but its first NNM is equivalent to its linear rigid body mode so $\left(\omega^{\mathrm{R}}(E)_1\right)^{\mathrm{B}} = 0$ and $\left(\phi^{\mathrm{R}}(E)_1\right)^{\mathrm{B}} = \begin{bmatrix}1 & 1\end{bmatrix}^{\mathrm{T}}$. The frequency dependence of its second RLMM, $\left(\omega^{\mathrm{R}}(E)_2\right)^{\mathrm{B}}$, is shown with a green line in Figure 7, ranging from 0.89 to 2.45 rad/s at E=10^5. The corresponding shape also happens to be constant with energy, $\left(\phi^{\mathrm{R}}(E)_2\right)^{\mathrm{B}} = \begin{bmatrix}1 & -1\end{bmatrix}^{\mathrm{T}}$. Now the procedure outlined in Figure 6 can be applied to predict the RLMMs of the assembled system. This was implemented using the freely available "ritzscomb" Matlab routine which implements the method described in [3, 15]. The frequency-energy curves for each of the RLMMs computed using this approach are shown in Figure 8.

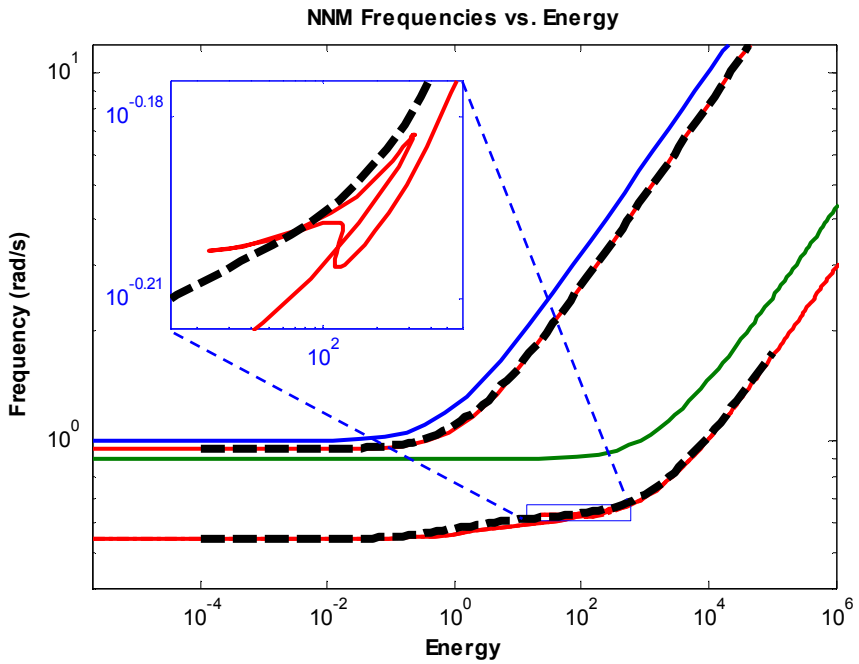

Figure 8: Frequency energy curves of the subcomponents and assembly shown in Figure 7. Blue: RLMM frequency of substructure A, Green: 2nd RLMM frequency of substructure B, Black Dashed: RLMM frequencies of the substructuring prediction using the method in Section 2.4, Red: True frequency-energy curves of the assembly, repeated from Figure 7.

Figure 8 shows that the RLMM method reproduces the nonlinear modes of the assembly with surprising accuracy. The RLMMs are linear models and they were assembled using linear substructuring techniques, so this results suggests that the frequency-energy dependence of the assembly is governed primarily by the effective natural frequencies (or RLMM frequencies) of the underlying substructures. Other nonlinear effects, such as nonlinear coupling between the underlying linear modes, seem to be much less significant. On the other hand, the inset shows that the linear RLMM model is incapable of describing the internal resonance that occurs when the energy is near E=100, so that feature of the response is completely missed.

In order to better understand how well the RLMM approximation captures the response of the nonlinear system, the first nonlinear normal mode of the assembly is shown in Figure 9 for an energy level of E=250. (Recall that the NNM is simply a periodic response of the nonlinear structure.) The corresponding response of the RLMM model is also shown, which is a pure cosine since the RLMM is a linear model. Comparing the curves, the RLMM can be seen to approximate the motion of $x_2(t)$ quite well; $x_2(t)$ dominates the response of this NNM at this energy level. On the other hand, the NNM shape of $x_1(t)$ is dominated by higher frequency motion that cannot be captured by the RLMM model.

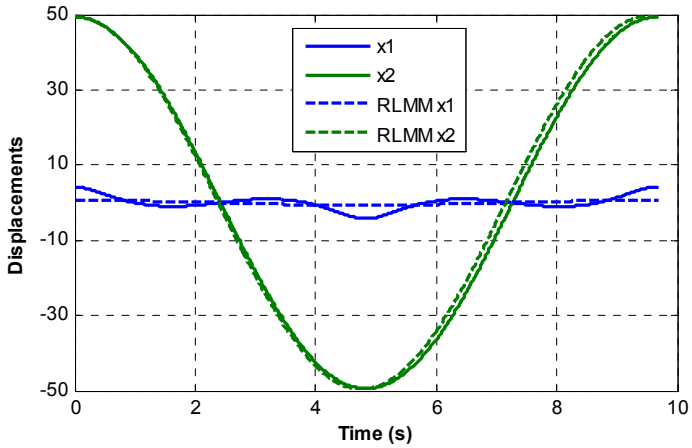

Figure 9: Periodic responses (e.g. NNM responses) of each degree of freedom for the true nonlinear assembly (solid lines) and the linear RLMM approximation (dashed lines).

3.3 Three Degree of Freedom Example of RLMM Substructuring

It was noted previously that both of the subcomponents used in the example in the previous subsection had constant RLMM mode shapes, and this might cause one to question whether those results were simply an anomaly arising because the mode shapes were constant. This was evaluated by using the RLMM substructuring procedure to add yet another copy of subsystem B to assembly described in Figures 7 and 8. The result, summarized in Figure 10 below, shows that once again very accurate results were obtained using the RLMM procedure, even though the shapes of the RLMM modes of one of the substructures changed very significantly in this second example.

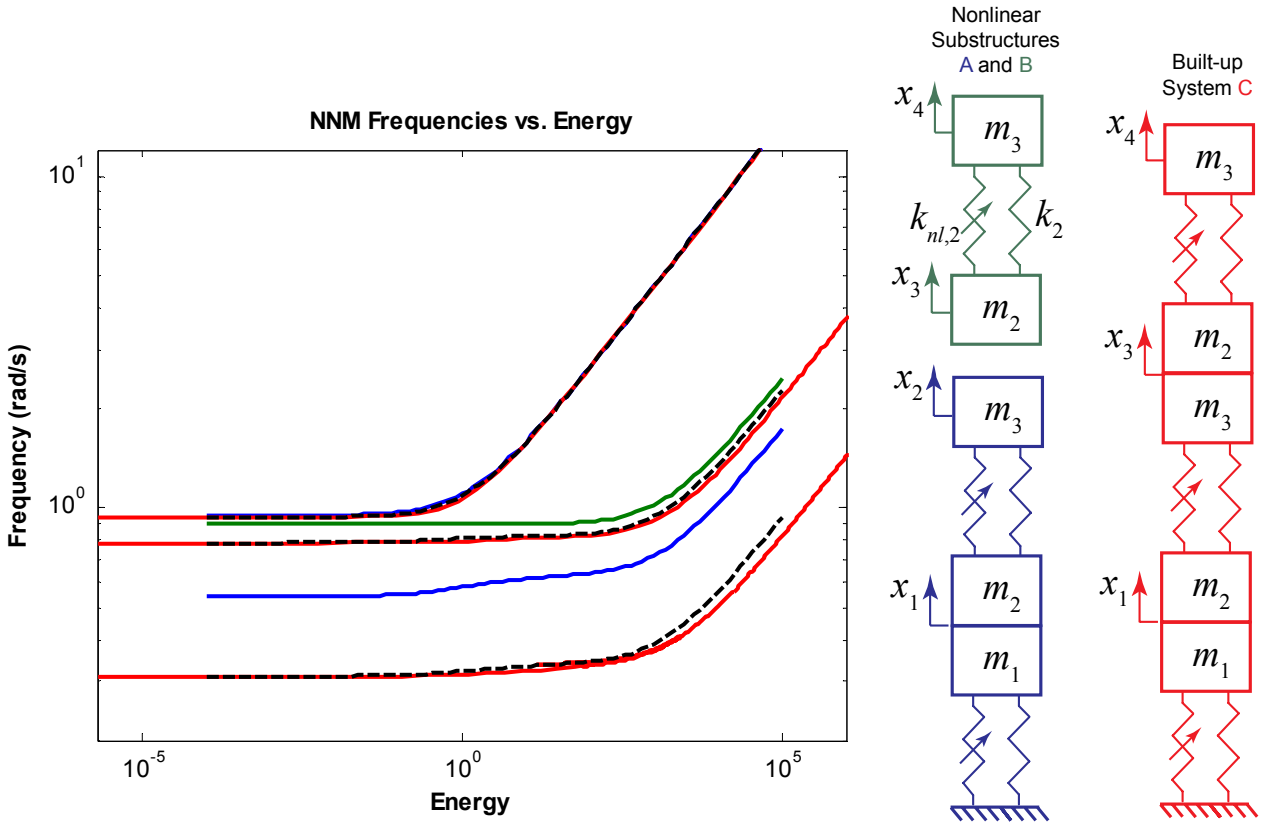

Figure 10: Nonlinear normal modes and RLMM approximations for a 3DOF substructuring problem. Substructure B in this example is the built-up system C in Figure 7.

It is important to note that the actual nonlinear normal modes of this system show several internal resonances which are not visible due to the coarse scale of the frequency-energy plot in Figure 10. Indeed, some effort was required to compute the true NNMs of this system since the 1st NNM curve suddenly doubles back upon itself several times. The RLMM method does not capture any of this complexity, but it does capture the overall trend in the NNM curves, and it does so at a miniscule computational cost compared to the rigorous nonlinear model.

4. Conclusions

This work has extended concepts from linear modal substructuring to assemblies of nonlinear subcomponents using the nonlinear normal mode concept. Nonlinear normal modes provide important insights into both the forced and free response of a system, and this work has shown that the basic evolution of the nonlinear normal modes of an assembly can be predicted very accurately if the NNMs of the subcomponents are known. Their evolution seems to be dominated by the frequency-energy dependence of the individual subcomponents, so concepts from linear substructuring can be readily applied to understand how each subcomponent contributes to the dynamic behavior of the assembly. Furthermore, these observations were exploited by presenting a new substructuring technique that uses linear modal substructuring techniques to assemble linear models for the subcomponents, here called Representative Linear Modal Models (RLMMs), in order to predict the frequency-energy dependence of the assembly. This method was found to predict the frequency-energy evolution very accurately and with minimal computational cost.

Of course, it is important to remember that linear models are not able to capture exclusively nonlinear phenomena such as internal resonance, instabilities or chaos, so any linear analysis should be followed by a more detailed nonlinear analysis at key energy levels in order to assure that important dynamics have not been missed. Fortunately, in many cases one can predict the energy levels at which internal resonances might occur based on the NNM curves. For example when a system has cubic springs, internal resonance typically occurs when one mode has a frequency that is three times that of another mode [18]. The first NNM in Figure 7 is three times the second at only one energy level, precisely that at which the internal resonance was observed. Hence, for a system such as this one could predict the general evolution of the NNMs using the substructure RLMMs and linear substructuring and then identify the energy at which internal resonances are possible.

Acknowledgements

The authors gratefully acknowledge the support of the Air Force Office of Scientific Research under grant number FA9550-11-1-0035, administered by the Dr. David Stargel of the Multi-Scale Structural Mechanics and Prognosis Program.

Appendix

This section explains how two linear substructures, each described by a set of linear modes can be joined so that the modes of the assembly can be computed. The natural frequencies, ω_r, and the matrix of mass-normalized mode shapes, $\mathbf{\Phi}$, are known for each substructure. The concatenated equations of motion (in second order form) are then the following.

$$\begin{bmatrix} \mathbf{I}_A & 0 \\ 0 & \mathbf{I}_B \end{bmatrix} \begin{Bmatrix} \ddot{\mathbf{q}}_A \\ \ddot{\mathbf{q}}_B \end{Bmatrix} + \begin{bmatrix} \left[\backslash \omega_r^2 \backslash \right]_A & \mathbf{0} \\ \mathbf{0} & \left[\backslash \omega_r^2 \backslash \right]_B \end{bmatrix} \begin{Bmatrix} \mathbf{q}_A \\ \mathbf{q}_B \end{Bmatrix} = \begin{Bmatrix} \mathbf{\Phi}_A{}^T \mathbf{F}_A \\ \mathbf{\Phi}_B{}^T \mathbf{F}_B \end{Bmatrix}$$
$$\begin{Bmatrix} \mathbf{y}_A \\ \mathbf{y}_B \end{Bmatrix} = \begin{bmatrix} \mathbf{\Phi}_A & \mathbf{0} \\ \mathbf{0} & \mathbf{\Phi}_B \end{bmatrix} \begin{Bmatrix} \mathbf{q}_A \\ \mathbf{q}_B \end{Bmatrix} \tag{8}$$

The constraints can then be expressed in terms of the physical or modal coordinates as follows.

$$\left[\mathbf{a}_p \right] \begin{Bmatrix} \mathbf{y}_A \\ \mathbf{y}_B \end{Bmatrix} = 0 \qquad \rightarrow \qquad \left[\mathbf{a}_p \right] \begin{bmatrix} \mathbf{\Phi}_A & 0 \\ 0 & \mathbf{\Phi}_B \end{bmatrix} \begin{Bmatrix} \mathbf{q}_A \\ \mathbf{q}_B \end{Bmatrix} = 0 \tag{9}$$

Then the constrained generalized coordinates can be eliminated by defining a nonsquare matrix **B** that transforms the concatenated coordinates into a set of unconstrained coordinates using either the method described in [15] or the method in [5] where

$$\begin{Bmatrix} \mathbf{q}_C \\ \mathbf{q}_A \end{Bmatrix} = \mathbf{B}\mathbf{q}_u \tag{10}$$

and **B** is in the null space of the matrix of constraints in eq. (9). The equations of motion of the system in unconstrained coordinates then become the following

$$\begin{aligned} \mathbf{M}_u\ddot{\mathbf{q}}_u + \mathbf{K}_u\mathbf{q}_u &= \mathbf{B}^T \begin{Bmatrix} \boldsymbol{\Phi}_A{}^T\mathbf{F}_A \\ \boldsymbol{\Phi}_B{}^T\mathbf{F}_B \end{Bmatrix} \\ \begin{Bmatrix} \mathbf{y}_A \\ \mathbf{y}_B \end{Bmatrix} &= \begin{bmatrix} \boldsymbol{\Phi}_A & \mathbf{0} \\ \mathbf{0} & \boldsymbol{\Phi}_B \end{bmatrix} \mathbf{B}\mathbf{q}_u \end{aligned} \tag{11}$$

where the mass and stiffness matrices of the coupled system are.

$$\mathbf{M}_u = \mathbf{B}^T \begin{bmatrix} \mathbf{I}_A & 0 \\ 0 & \mathbf{I}_B \end{bmatrix} \mathbf{B}, \qquad \mathbf{K}_u = \mathbf{B}^T \begin{bmatrix} \left[\backslash \omega_r^2 \backslash\right]_A & \mathbf{0} \\ \mathbf{0} & \left[\backslash \omega_r^2 \backslash\right]_B \end{bmatrix} \mathbf{B} \tag{12}$$

One can show that multiplying the forces by $\mathbf{B}^T$ eliminates the constraint forces, ensuring that compatibility is satisfied (see chapter 9 in [15]). The modes of the assembly can then be computed by solving an eigenvalue problem with $\mathbf{M}_u$, $\mathbf{K}_u$ and then relating the mode shapes in $\mathbf{q}_u$ coordinates back to the physical coordinates with eq. (11).

References

[1] R. R. J. Craig and M. C. C. Bampton, "Coupling of Substructures Using Component Mode Synthesis," *AIAA Journal,* vol. 6, pp. 1313-1319, 1968.

[2] M. S. Allen, H. M. Gindlin, and R. L. Mayes, "Experimental Modal Substructuring to Estimate Fixed-Base Modes from Tests on a Flexible Fixture," *Journal of Sound and Vibration,* vol. 330, pp. 4413-4428, 2011.

[3] M. S. Allen, R. L. Mayes, and E. J. Bergman, "Experimental Modal Substructuring to Couple and Uncouple Substructures with Flexible Fixtures and Multi-point Connections," *Journal of Sound and Vibration,* vol. 329, pp. 4891–4906, 2010.

[4] M. S. Allen, D. C. Kammer, and R. L. Mayes, "Metrics for Diagnosing Negative Mass and Stiffness when Uncoupling Experimental and Analytical Substructures," in *29th International Modal Analysis Conference (IMAC XXIX)* Jacksonville, Florida, 2011.

[5] D. de Klerk, D. J. Rixen, and S. N. Voormeeren, "General framework for dynamic substructuring: History, review, and classification of techniques," *AIAA Journal,* vol. 46, pp. 1169-1181, 2008.

[6] F. Bourquin, "Analysis and comparison of several component mode synthesis methods on one-dimensional domains," *Numerische Mathematik,* vol. 58, pp. 11-34, 1990.

[7] M. S. Allen, D. C. Kammer, and R. L. Mayes, "Uncertainty in Experimental/Analytical Substructuring Predictions: A Review with Illustrative Examples," in *ISMA2010 - International Conference on Noise and Vibration Engineering* Leuven, Belgium, 2010.

[8] R. M. Rosenberg, "Normal modes of nonlinear dual-mode systems," *Journal of Applied Mechanics,* vol. 27, pp. 263–268, 1960.

[9] G. Kerschen, M. Peeters, J. C. Golinval, and A. F. Vakakis, "Nonlinear normal modes. Part I. A useful framework for the structural dynamicist," *Mechanical Systems and Signal Processing,* vol. 23, pp. 170-94, 2009.

[10] A. F. Vakakis, "Non-linear normal modes (NNMs) and their applications in vibration theory: an overview," *Mechanical Systems and Signal Processing,* vol. 11, pp. 3-22, 1997.

[11] M. Peeters, R. Viguie, G. Serandour, G. Kerschen, and J. C. Golinval, "Nonlinear normal modes, part II: toward a practical computation using numerical continuation techniques," *Mechanical Systems and Signal Processing,* vol. 23, pp. 195-216, 2009.

[12] C. R. Pickrel, "Airplane ground vibration testing: Correlation with nominal modal model," in *20th International Modal Analysis Conference (IMAC-XX)* Los Angeles, CA, 2002.
[13] J.-J. E. Slotine and W. Li, *Applied Nonlinear Control*. Upper Saddle River, New Jersey: Prentice Hall, 1991.
[14] J. H. Ginsberg, *Engineering Dynamics*, 3rd ed. Cambridge, MA: Cambridge University Press, 2005.
[15] J. H. Ginsberg, *Mechanical and Structural Vibrations*, First ed. New York: John Wiley and Sons, 2001.
[16] J. S. Bay, *Fundamentals of Linear State Space Systems*. Boston: McGraw-Hill, 1999.
[17] M. W. Sracic and M. S. Allen, "Method for Identifying Models of Nonlinear Systems Using Linear Time Periodic Approximations," *Mechanical Systems and Signal Processing,* vol. 25, pp. 2705-2721, 2011.
[18] A. H. Nayfeh, *Introduction to perturbation techniques*. New York: Wiley, 1981.
[19] M. W. Sracic and M. S. Allen, "Numerical Continuation of Periodic Orbits for Harmonically Forced Nonlinear Systems," in *29th International Modal Analysis Conference (IMAC XXIX)* Jacksonville, Florida, 2011.
[20] M. B. Ozer, H. N. Ozguven, and T. J. Royston, "Identification of structural non-linearities using describing functions and the Sherman-Morrison method," *Mechanical Systems and Signal Processing,* vol. 23, pp. 30-44, 2009.
[21] P. Apiwattanalunggarn, S. W. Shaw, and C. Pierre, "Component mode synthesis using nonlinear normal modes," *Nonlinear Dynamics,* vol. 41, pp. 17-46, 2005.
[22] L. Meirovich, *Fundamentals of Vibrations*. New York, NY: McGraw-Hill, 2001.
[23] A. F. Vakakis, D. M. McFarland, L. Bergman, L. I. Manevitch, and O. Gendelman, "Isolated Resonance Captures and Resonance Capture Cascades Leading to Single- or Multi-Mode Passive Energy Pumping in Damped Coupled Oscillators," *Journal of Vibration and Acoustics,* vol. 126, pp. 235-244, 2004.